SANDIA REPORT

SAND2016-9472
Unlimited Release
Printed September 2016

Wavelength Conversion Arrays for Optical and X-Ray Diagnostics at Z

Erik J. Skogen, Daniel H. Dolan III, G. Allen Vawter, Anna Tauke-Pedretti, Charles Alford, Florante G. Cajas

Prepared by
Sandia National Laboratories
Albuquerque, New Mexico 87185 and Livermore, California 94550

Sandia National Laboratories is a multi-mission laboratory managed and operated by Sandia Corporation, a wholly owned subsidiary of Lockheed Martin Corporation, for the U.S. Department of Energy's National Nuclear Security Administration under contract DE-AC04-94AL85000.

Issued by Sandia National Laboratories, operated for the United States Department of Energy by Sandia Corporation.

Available to DOE and DOE contractors from
U.S. Department of Energy
Office of Scientific and Technical Information
P.O. Box 62
Oak Ridge, TN 37831

Telephone: (865) 576-8401
Facsimile: (865) 576-5728
E-Mail: reports@osti.gov
Online ordering: http://www.osti.gov/scitech

Available to the public from
U.S. Department of Commerce
National Technical Information Service
5301 Shawnee Rd
Alexandria, VA 22312

Telephone: (800) 553-6847
Facsimile: (703) 605-6900
E-Mail: orders@ntis.gov
Online order: http://www.ntis.gov/search

SAND2016-9472
Unlimited Release
09/2016

Wavelength Conversion Arrays for Optical and X-Ray Diagnostics at Z

Erik J. Skogen, Daniel H. Dolan III, G. Allen Vawter, Anna Tauke-Pedretti, Greg Peake, Charles Alford, Florante G. Cajas

1764, 1646
Sandia National Laboratories
P.O. Box 5800
Albuquerque, New Mexico 87185-MS1085

Abstract

Optical diagnostics play a central role in dynamic compression research. Currently, streak cameras are employed to record temporal and spectroscopic information in single-event experiments, yet are limited in several ways; the tradeoff between time resolution and total record duration is one such limitation. This project solves the limitations that streak cameras impose on dynamic compression experiments while reducing both cost and risk (equipment and labor) by utilizing standard high-speed digitizers and commercial telecommunications equipment. The missing link is the capability to convert the set of experimental (visible/x-ray) wavelengths to the infrared wavelengths used in telecommunications.

In this report, we describe the problem we are solving, our approach, our results, and describe the system that was delivered to the customer. The system consists of an 8-channel visible-to-infrared converter with > 2 GHz 3-dB bandwidth.

CONTENTS

FIGURES

TABLES

NOMENCLATURE

AWG	arrayed waveguide grating
COTS	commercial of the shelf
CW	continuous wave
dB	decibel
EAM	electro-absorption modulator
DOE	Department of Energy
GHz	gigahertz
GSPS	giga-samples per second
PD	photodiode
SNL	Sandia National Laboratories
QWI	quantum well intermixing

1. INTRODUCTION

Optical diagnostics play a central role in dynamic compression research. Currently, streak cameras are employed to record temporal and spectroscopic information in single-event experiments. Optical signals streaked by the camera create a two-dimensional record of the event, obtaining high temporal and spatial (spectrographic) resolution over relatively short time scales (0.1-10 μs). These measurements are not easily achieved, however; equipment costs limit the experimental versatility, and limited readout elements constrain the tradeoff between temporal resolution and time duration. Furthermore, these cameras are at risk of becoming unsupported.

This project will solve the limitations that streak cameras impose on dynamic compression experiments while reducing both cost and risk (equipment and labor) by utilizing standard high-speed digitizers and commercial telecommunications equipment. The missing link is the capability to convert the set of experimental (visible/x-ray) wavelengths to the infrared wavelengths used in telecommunications. Although infrared-to-infrared wavelength converters exist, the concept has not applied to visible-to-infrared conversion technology. In fact, there are many ways of translating light from one optical wavelength to another [1], but few are useful for recording information in a broad spectrum measurement. Nonlinear techniques are wavelength specific (e.g., 1064 nm to 532 nm) and demand far more optical power than found in a spectroscopic measurement [2]. Semiconductor switching [3] can be used to translate visible/ultraviolet information onto an infrared carrier, but the technique is not sensitive enough to detect ~mW power levels emitted by samples in narrow spectral band. Commercial wavelength conversion devices exist for coupling between telecommunications networks (e.g., 1550 nm to 1551 nm), and there is extensive research in this area [4-6]. Most of this effort, however, is aimed at infrared-to-infrared conversion, not the shorter wavelengths of interest here.

The Sandia team aims to enable the transition from decades-old streak camera techniques to modern technology using high-speed digitizers and fiber-optic components tailored for dynamic compression experiments. This transition has the potential to break the tradeoff between temporal resolution and time duration as the digitizers have the capability to store 100 times more data than streak cameras; the temporal resolution and dynamic range of the wavelength converter must be explored, assessed, and engineered to meet the challenging experimental metrics. We leveraged the expertise of Sandia's photonic integrated circuit technology to develop a linear array of visible-to-infrared wavelength conversion circuits that met the needs of the program. The Sandia team has bridged the technological gaps to create the solution, which also shows a clear path toward reducing cost and risk, while improving experimental capability and versatility.

Measurement systems utilizing high-speed digitizers and commercially available telecommunications equipment have already enabled vast improvements in sensitivity and configurability of velocimetry experiments. A similar approach aimed at optical pyrometry will enable similar benefits to be realized.

To devise a system with greater capability, it is important to understand the function of streak cameras within the context of the measurement. Streak cameras store information in a two-dimensional format, where one axis represents time and the other position/wavelength. The total information recorded in this format is proportional to the number of readout elements, which is on the order of 1 million points (1024 x 1024 pixels). Theoretically, streak cameras can record thousands of channels simultaneously, though in practice only 100-200 truly independent measurements are possible. The effective bandwidth of a streak camera may be quite large, but there is a tradeoff between time resolution and total duration. For example, a 500 nanosecond streak over 1000 pixels is functionally similar to 2 gigasamples per second (GSPS) digitizer, but information is typically blurred over several pixels. Practically speaking, the limiting rise time (response to a discontinuous change) in this situation is on the order of 5 nanoseconds (<1 gigahertz bandwidth). Time resolution can be improved by increasing streak rate, but this reduces the total recorded duration. By comparison, a modern digitizer can record many GSPS at input frequencies of several GHz, storing 25 million points per channel over four channels (1 million points), upgradeable to 250 million points per channel (1 billion points). As such, a digitizer can store 100-1000 times more information than a streak camera, a substantial capability improvement.

.

2. SYSTEM ARCHITECTURE

High-speed digitizers offer an attractive alternative to streak cameras, and other measurement systems have benefited handsomely from the combination of digitizers with commercial telecommunications equipment. However, digitizers typically have 4-8 channels, whereas spectroscopy measurements require a greater number of simultaneous measurements. Time-division multiplexing, where a single channel records simultaneous optical measurements sequentially, can be used to mimic the parallelism of a streak camera measurement. To do so, each measurement must be time delayed by an amount slightly longer than the measurement itself (~1000 nanoseconds). Such delays are feasible at wavelengths near the silica transmission peak centered (~1550 nm), but impractical in the visible spectrum because of higher (100 times) fiber attenuation. Furthermore, telecommunications components are designed for use at infrared wavelengths and will not perform in the visible.

A visible-to-infrared wavelength converter is the missing link that would enable construction of novel measurement system for dynamic materials experiments. There has been a great deal of work on wavelength conversion techniques in the telecommunications world, and the photonic integrated circuit experts at Sandia have a great deal of experience with such technology. However, until now, there has not been an application need for visible-to-infrared wavelength conversion technology. We have leveraged the existing technology base to create the needed solution.

Figure 1 depicts the use of wavelength conversion in high-speed spectroscopy. Light generated during the experiment is captured by a large core optical fiber. This fiber delivers the spectrum to a dispersive element, such as a diffraction grating, to spatially separate wavelengths. These wavelengths are then converted to infrared signals with a known transfer function. Each infrared channel is sequentially delayed in time using appropriate lengths of optical fiber and recombined using an arrayed waveguide grating (AWG) before being detected and digitized by a high-speed oscilloscope. Once recorded, the data can be reassembled in the digital domain, applying the appropriate filters and corrections.

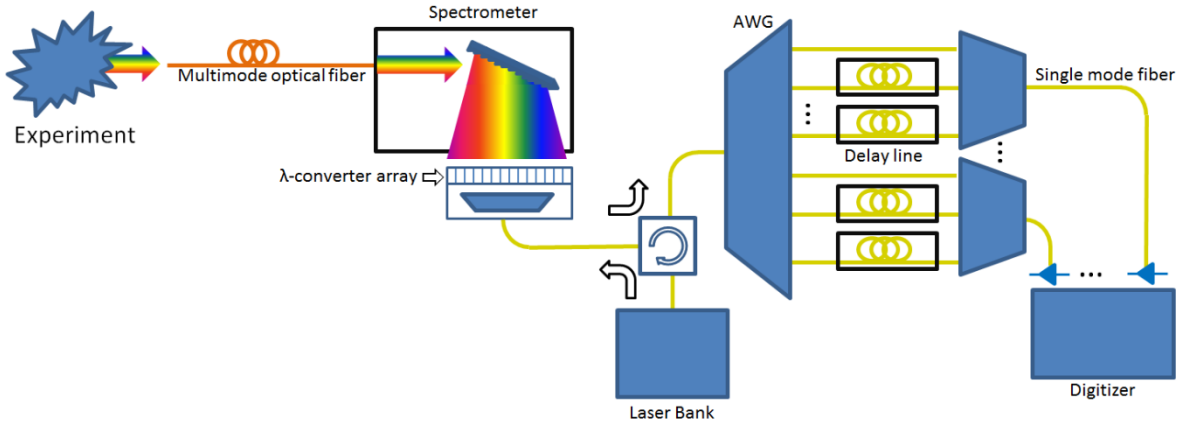

Figure 1. Measurement system architecture.

The visible-to-infrared wavelength converter relies on Sandia's unique state-of-the-art photonic integrated circuit fabrication platform, which enables monolithic integration of >10 unique opto-electronic components on a single chip. The optical wavelength converter exploits this technology and is comprised of two opto-electronic active components: the photodiode (PD) and electroabsorption modulator (EAM). The PD is a light-to-current transducer; while the EAM is a voltage dependent transmission switch (higher reverse voltage leads to lower light transmission).

The wavelength converter requires the EAM and PD to be within close proximity for low-latency and high-bandwidth, and the EAM operates with metrics surpassing the output saturation power and extinction efficiency of COTS components. The PD is mounted on an AlN submount which is then mounted onto a printed circuit board used to fan-out the individual channels for subsequent amplification. This architecture offers flexible detector selection that can be tailored to needs of a particular measurement. For example, using the same wavelength converter base, a detector sensitive to visible light could be exchanged for one sensitive to x-rays.

The infrared laser channels are supplied by a bank of discrete telecom lasers which can be combined onto a single optical fiber. This fiber can then be passed through a circulator such that the continuous-wave (CW) light is directed toward the EAM array where it is de-multiplexed and modulated by the signal received by the PD. The modulated infrared light is then multiplexed back onto the single fiber and passes through the circulator again, this time directed toward a system used to temporally delay each channel such that several channels can be sequentially recorded by the digitizer.

Figure 2 shows a schematic of a single wavelength converter channel. The dispersed visible input signal is received by the PD, which is DC biased using a bias-t. The signal is then electrically amplified by a two-stage amplifier before passing through another bias-t to drive the modulator. The modulator receives a CW infrared beam, the data is transcribed, and a modulated infrared signal is sent back on the same optical fiber.

There are several challenges that must be overcome to successfully demonstrate an efficient, high-fidelity wavelength converter channel. First, the proximity of the PD to the EAM is of crucial importance as radio-frequency parasitic effects will degrade device performance.

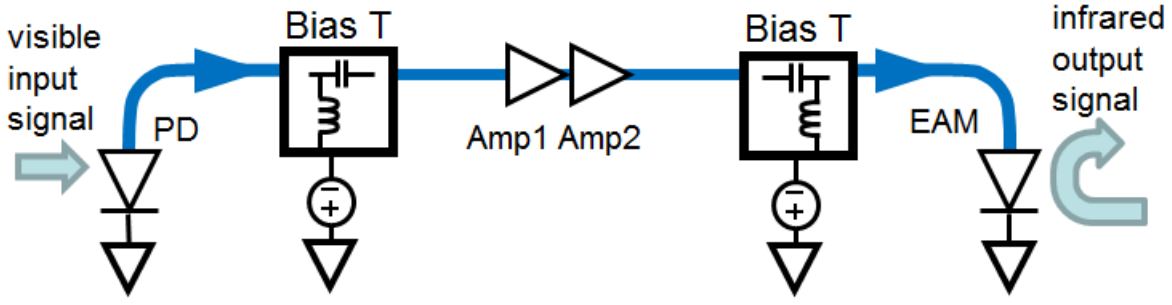

Figure 2. Schematic of a single wavelength channel. The dispersed visible input signal is received by the PD, which is DC biased using a bias-t, the signal is then electrically amplified by a two-stage amplifier before passing through another bias-t to drive the modulator. The modulator receives a CW infrared beam, the data is transcribed, and a modulated infrared signal is sent back on the same optical fiber.

Second, characteristics of the PD will set the dynamic range and the bandwidth of the device and must be selected with care. Thirdly, the length of the EAM will play a large role in the efficiency and signal integrity. As is evident a large variety of interdependencies must be managed to successfully demonstrate a useful device. To this end we have made extensive use of a range of modeling software.

Our approach to achieving a new measurement system, outlined above, can be categorized into two main components: system design/specification, and wavelength converter design/fabrication/testing. The system design and specification consisted of documenting the requirements of the system to meet the goals of the overall experiment. The system specifications were developed in coordination with the design of the wavelength converter to ensure that the desired metrics could be met. Modeling and simulation of the wavelength converter device was extensively utilized to design and improve upon device designs.

The second stage focused on fabrication and testing of the individual wavelength converter devices. After completing the system specifications, the metrics for the EAM, PD, and amplification stages were set and the component design was started. For the PD we found that the available COTS devices were sufficient to demonstrate the prototype system. However, the system sensitivity could be improved with a custom solution. The EAM required a custom solution to achieve the high extinction efficiency to deliver the specified extinction using a relatively low input drive voltage. The amplification stages are required to amplify the signal received by the PD to deliver the appropriate drive voltage to the EAM.

The system specification was developed in accordance to the end application and is summarized in the following table. As the project proceeded several of the design targets were necessarily changed. The number of channels was reduced from 32 to 8 for prototyping; the number of channels can be increased by scaling the solution. The minimum instantaneous input frequency was changed from DC to ~5 kHz to allow for AC coupling of the electrical amplifiers.

Table 1. System specifications

Parameter	Description	Design Target
N	Number of channels	32 changed to 8
λ_c (nm)	Channel spectral width	10
λ_w (nm)	Spectral width	400-720
$P_{c\text{-}min}$ (W)	Minimum optical power to record in each channel	10e-6
$P_{c\text{-}max}$ (W)	Maximum optical power to record in each channel	10e-3
f_{min} (Hz)	Minimum instantaneous input frequency	DC changed to 5 kHz
f_{max} (Hz)	Maximum instantaneous input frequency	2e9

3. RESULTS

This section documents the main findings of this program and is broken into three main parts. First, the design and simulation of the electroabsorption modulator will be described. Next, the design and test results of electrical amplification stages will be described. Finally, the system level assembly and test will be described.

The electroabsorption modulator is a critical component of the wavelength conversion system. It is responsible for transcribing data in the electrical domain to the infrared optical domain. The EAM device is comprised of several components, a passive input/output waveguide, a section for absorption modulation through the quantum-confined Stark effect, and a reflector. The modulator is a diode and functions by applying an external voltage, which generates an electric field across the intrinsic region and changes the absorption coefficient. As light is absorbed by the modulator photo-current is generated that must be extracted through the contacts. The modulator is epitaxially grown and care must be taken to avoid excessive photo-carrier accumulation which will degrade device performance through the carrier screening effect which manifests itself as a reduction in device RF bandwidth. The epitaxial band structure of the modulator was modeled and designs were identified that result in more efficient extraction of photo-current, that is, efficient transport of the carriers to the contacts. The results are shown in Fig. 3, where in Fig 3a, an epitaxial design is shown that has significant potential barriers at the heterointerfaces which impede carrier transport and results in a carrier accumulation at those positions. In Fig. 3b, an improved design is shown which includes a step-wise grade of the band

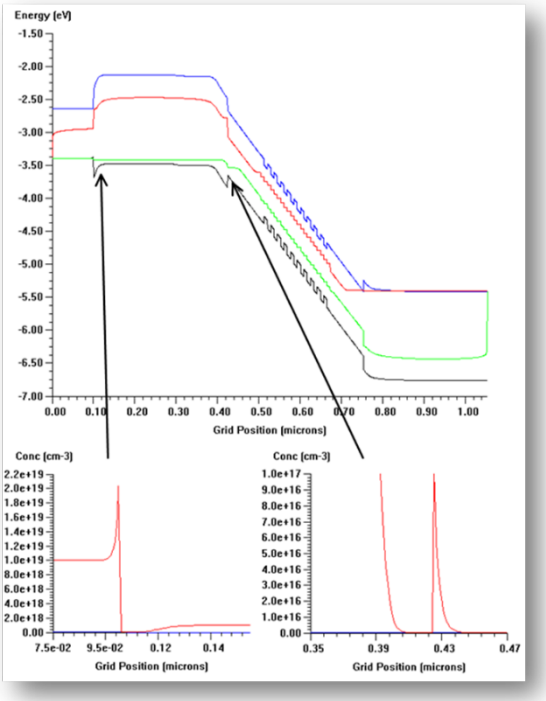

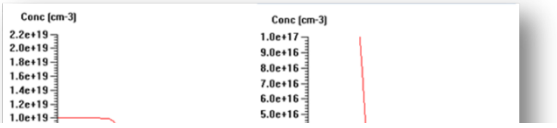

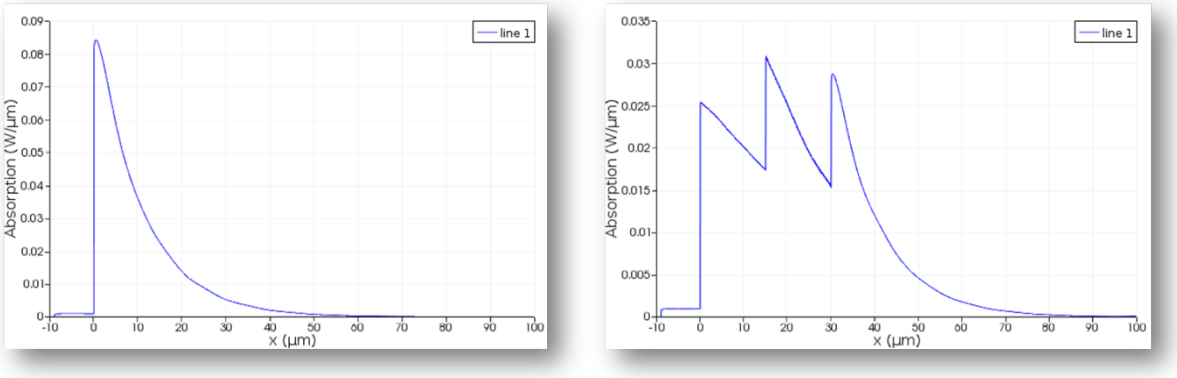

(a) (b)

Figure 4. Optical absorption as a function of longitudinal modulator length. The modulator device starts at 0 µm and extends to 100 µm.

gap resulting in a simulation with nearly an order of magnitude reduction in the carrier accumulation.

Another innovation was achieved in the modulator design which resulted in a patent application. This innovation involves the tailoring of the band gap along the longitudinal length of the device such that the absorption at the light input is initially relatively low and gradually increases along the length of the device. We were able to accomplish this using a multistep quantum well intermixing (QWI) process. The QWI process, in this case, is used to increase the band gap in a particular region and thus reduce the absorption in that region as opposed to the non-intermixed region [7-8]. We modeled this absorption as a function of length and found that by tailoring the absorption along the length of the device we could create a more uniform absorption profile, as shown in Fig. 4. This reduction of absorption at the optical input will prevent a photo-carrier build-up near the optical input, which, as described previously, can lead to reduced performance. The more uniform optical absorption will lead to a more uniform distribution of photo-carrier generation and an improvement in performance under high optical intensity. This enhanced performance under high optical intensity translates to an improved link gain, since link gain is proportional to the square of the input optical power.

Another component in the optical conversion array system is the amplification and bias stage that resides between the PD and the EAM. This stage serves to both amplify the received experimental signal from PD, and enables the PD and EAM to be DC biased to achieve optimal performance. First we will discuss the bias requirements for both the PD and EAM. Photodiodes commonly require a reverse DC bias to improve the carrier sweep out and to expand the intrinsic region which enables both higher optical power handling and lower capacitance over unbiased devices. A lower capacitance, for a lumped element device, enables a higher RF bandwidth to be achieved. Similarly for the EAM, a reverse bias also aids in carrier sweep out and lowers capacitance, but also is used to adjust the operating point on the extinction curve to the optimal position for the application whether it be for low insertion loss or high extinction efficiency. Commonly, these bias-ts are found in a stand-alone package which would add a considerable amount of bulk. Our solution was to use surface mount bias-ts and integrate them

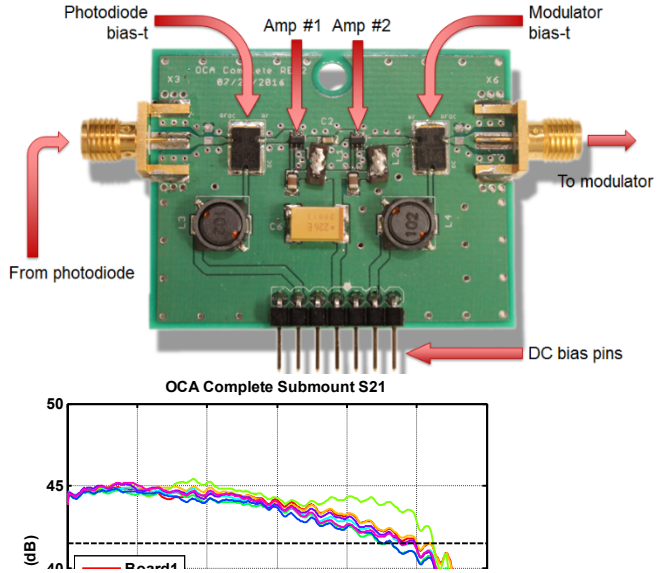

onto the printed circuit board, which saves ~10x or more in volume. Between the bias-ts we have the high-speed electrical amplifiers. These amplifiers are AC coupled and provide 22-23 dB of gain with a noise figure of 3.5 dB at 2 GHz. We used to of these amplifiers to achieve 44.5 dB of gain with a bandwidth of 2.5 GHz. A photo of the bias-t/amplifier PCB is shown in Fig. 5. The through response was measured using a network analyzer and is shown in Fig. 6. In the figure it is clear that the boards from all 8 channels are very similar, as expected, and achieve a smooth roll-off at 2.5 GHz.

To meet the objective of detection and conversion of 0.001 – 1 mW input optical power, we need to ensure that the voltage swing applied to the modulator is greater than 1 V peak-to-peak. To prove that we have achieved this goal an experiment was conducted using the PD and channel amplifier PCB. A diagram of the experimental setup is shown in Fig. 6. In this experiment the

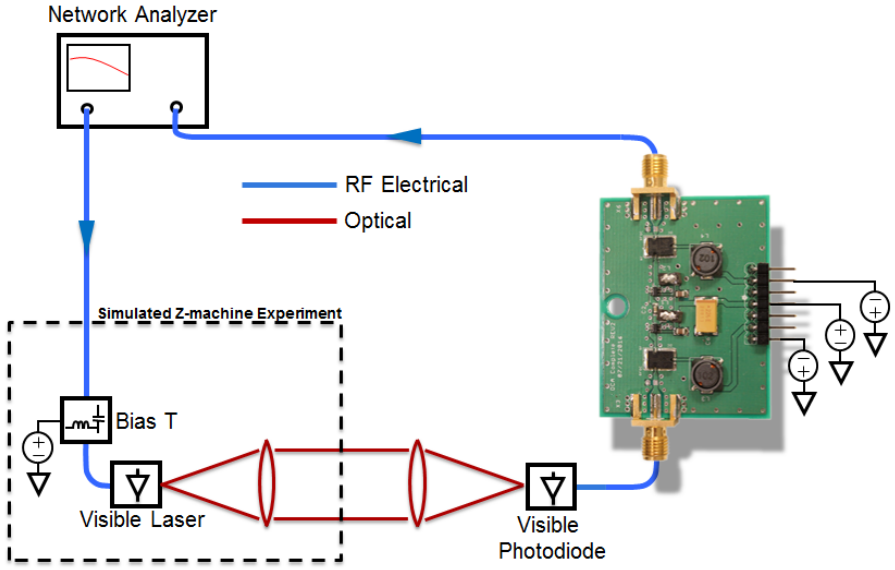

Figure 6. Experimental test set to measure the output voltage given the input optical power range of 0.001 – 1.0 mW.

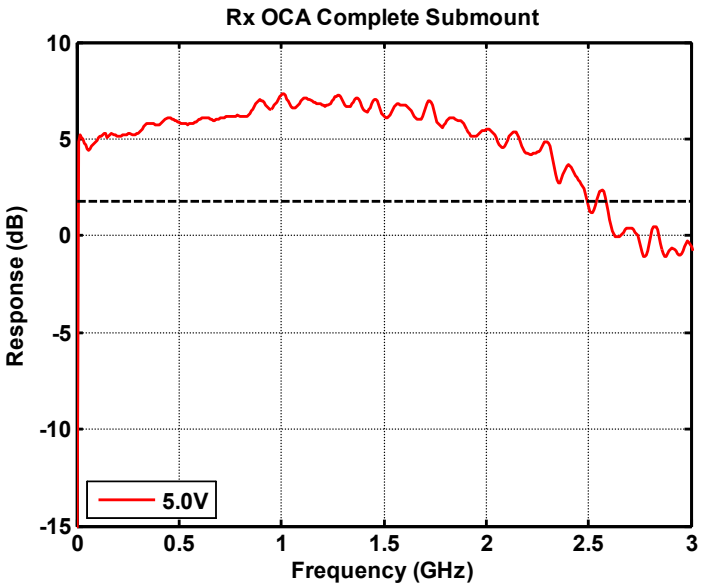

Figure 7. Experimental result of the receive function. The graph shows the signal that will be applied to the EAM using an input optical power modulation range of 0.001 – 1.0 mW.

visible laser was set to modulate between 0.1x the threshold current to 1 mW. The PD received this modulated light and amplified the signal. The amplified signal was then measured using a network analyzer. The results, shown in Fig. 7, indicate that the signal received by the network analyzer was at or above 5 dBm out to 2 GHz. This translates to a modulated voltage into 50 ohms of greater than 1.1 V peak-to-peak. The goal was achieved and the EAM should have enough voltage swing to achieve the infrared modulation goal.

Finally, the wavelength conversion system was constructed. Several PCBs were used to aid in the biasing and routing of the channel signals. First, the PD was mounted on an AlN submount which was subsequently soldered to a fan-out PCB. Each channel of the fan-out PCB was connected to a bias-t/amplifier line card. Each line card receives DC bias from a signal routing PCB. The RF output of the line cards connect to a fan-in PCB where the EAM array resides. An additional voltage regulator PCB sets and delivers the DC bias to each PD, EAM, and the set amplifiers, 18 voltage regulators in all. The voltage regulator PCB also monitors the photocurrent of each PD and EAM and displays the result on a panel meter. The system only needs -12 V, +12 V, and ground to operate, and is shown in Fig. 8.

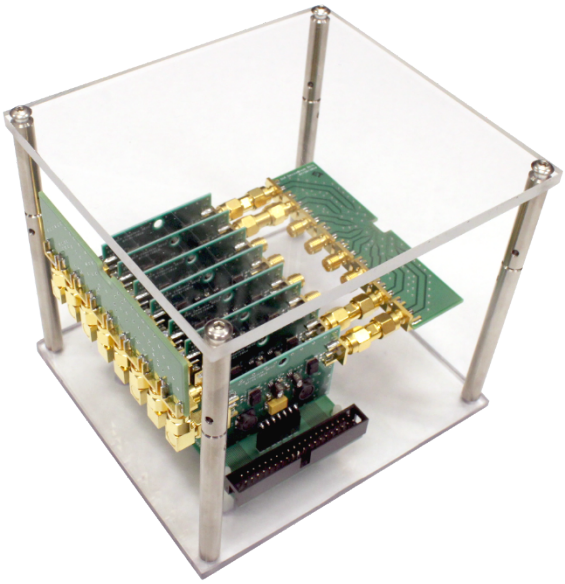

(a)

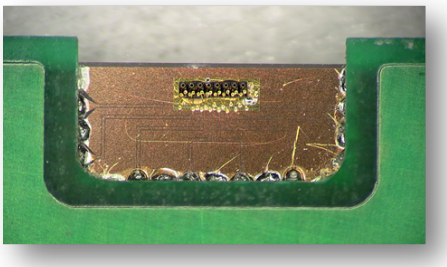

(b)

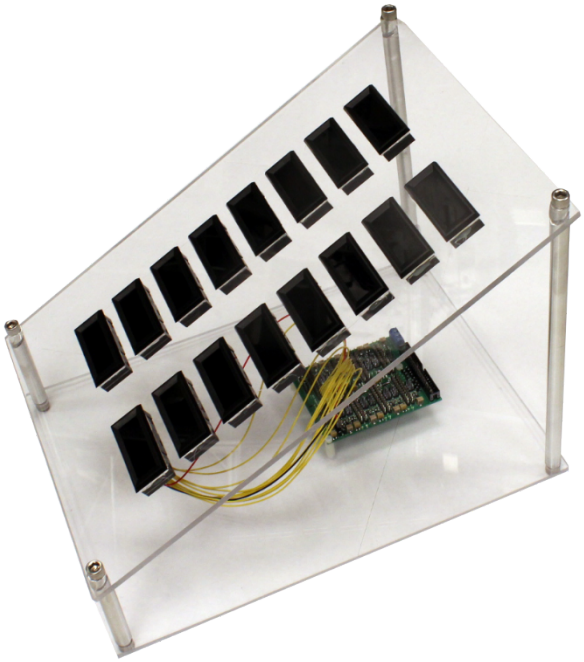

(c)

Figure 8. Optical wavelength conversion system. a) Module containing the PD, EAM, and bias/amplifier arrays. b) Photodiode array mounted and wire bonded to AlN submount and AlN submount soldered to the fan-out PCB. c) The power supply and read out module, voltage regulator PCB and panel meters.

4. CONCLUSIONS

The overarching goal of this project was to create a new capability for observing and recording dynamic materials experiments at Z. At the conclusion of the project a new prototype measurement system exists that not only mitigates the cost and risk associated with streak cameras, but adds significant new versatility in the measurement apparatus. Central to this goal was the development and demonstration of visible-to-infrared wavelength conversion arrays that meet or surpass requirements for visible spectroscopy: 8+ wavelength channels recorded over several microseconds with >2 GHz bandwidth. The number of channels in the array and their bandwidth/sensitivity are relevant to pyrometry/reflectivity measurements in dynamic compression experiments. We have a viable path to manufacturing many systems and/or scaling to larger number of channels and establish the cost/time of manufacture.

Wavelength conversion devices are directly related to dynamic temperature measurements, which are desperately needed for equation of state development and phase transition studies crucial to extending stockpile lifetime. The results of this project will revolutionize the quantity and quality of temperature measurements, offering a new approach to high-speed optical and x-ray measurements. This unique diagnostic approach bypasses the restrictions of existing technology, strengthening the science and technology base of the national laboratories.

5. REFERENCES

[1] Yoo, S.J.B., 'Wavelength Conversion Technologies for WDM Network Applications,' *J. Lightwave Tech*., vol. 14, pp. 955-966, 1996.

[2] Dunham, G. *et al*., 'Diagnostic methods for time-resolved optical spectroscopy of shocked liquid deuterium', *Rev. Sci. Instrum.*, vol 75, pp. 928-935, 2004.

[3] Saito, M. *et al*., 'Development of an all-optical infrared modulator and its application to fiber optic thermometry', *Rev. Sci. Instrum.*, vol 74, pp. 3832, 2003.

[4] Nicholes, S., *et al*., 'An 8x8 InP Monolithic Tunable Optical Router (MOTOR) Packet Forwarding Chip,' *J. Lightwave Tech*., vol. 28, pp. 641-650, 2010.

[5] Bernasconi, P. *et al*., 'Monolithically Integrated 40-gb/s Switchable Wavelength converter,' *J. Lightwave Tech*., vol. 24, pp. 71-76, 2006.

[6] Masanovic, M., *et al*., 'Widely Tunable Monolithically Integrated All-Optical Wavelength Converters in InP,' *J. Lightwave Tech*., vol. 23, pp. 1350-1362, 2005.

[7] Skogen, E. J., *et al*., "Monolithically Integrated Active Components: A Quantum Well Intermixing Approach," *IEEE J. Sel. Topics in Quantum Electron.*, vol. 11, pp. 343-355, 2005.

[8] Raring, J.R., *et al*., 'Design and Demonstration of Novel Quantum Well Intermixing Scheme for the Integration of UTC-Type Photodiodes with QW-Based Components," *IEEE J. Quantum Electron.*, vol. 42, pp. 171-181, 2006.

DISTRIBUTION

4 Lawrence Livermore National Laboratory
Attn: N. Dunipace (1)
P.O. Box 808, MS L-795
Livermore, CA 94551-0808

1	MS0359	D. Chavez, LDRD Office	1911
2	MS0899	Technical Library	9536 (electronic copy)
3	MS1085	Erik J. Skogen	1764


Sandia National Laboratories